

# Consistent Data Assimilation of Structural Isotopes: $^{23}\text{Na}$ and $^{56}\text{Fe}$

G. Palmiotti  
H. Hiruta  
M. Salvatores

September 2010



The INL is a U.S. Department of Energy National Laboratory  
operated by Battelle Energy Alliance

# **Consistent Data Assimilation of Structural Isotopes: $^{23}\text{Na}$ and $^{56}\text{Fe}$**

**G. Palmiotti  
H. Hiruta  
M. Salvatores**

**September 2010**

**Idaho National Laboratory  
Idaho Falls, Idaho 83415**

**<http://www.inl.gov>**

**Prepared for the  
U.S. Department of Energy  
Office of Science  
Under DOE Idaho Operations Office  
Contract DE-AC07-05ID14517**

#### **DISCLAIMER**

This information was prepared as an account of work sponsored by an agency of the U.S. Government. Neither the U.S. Government nor any agency thereof, nor any of their employees, makes any warranty, expressed or implied, or assumes any legal liability or responsibility for the accuracy, completeness, or usefulness, of any information, apparatus, product, or process disclosed, or represents that its use would not infringe privately owned rights. References herein to any specific commercial product, process, or service by trade name, trade mark, manufacturer, or otherwise, does not necessarily constitute or imply its endorsement, recommendation, or favoring by the U.S. Government or any agency thereof. The views and opinions of authors expressed herein do not necessarily state or reflect those of the U.S. Government or any agency thereof.

## SUMMARY

A new approach is proposed, the consistent data assimilation, that allows to link the integral data experiment results to basic nuclear parameters employed by evaluators to generate ENDF/B point energy files in order to improve them. Practical examples are provided for the structural materials  $^{23}\text{Na}$  and  $^{56}\text{Fe}$ . The sodium neutron propagation experiments, EURACOS and JANUS-8, are used to improve via modifications of  $^{23}\text{Na}$  nuclear parameters (like scattering radius, resonance parameters, Optical model parameters, Statistical Hauser-Feshbach model parameters, and Preequilibrium Exciton model parameters) the agreement of calculation versus experiments for a series of measured reaction rate detectors slopes. For the  $^{56}\text{Fe}$  case the EURACOS and ZPR3 assembly 54 are used. Results have shown inconsistencies in the set of nuclear parameters used so that further investigation is needed. Future work involves comparison of results against a more traditional multigroup adjustments, and extension to other isotope of interest in the reactor community.

## CONTENTS

1.	INTRODUCTION .....	1
2.	THEORY .....	1
2.1	Consistent Data Assimilation Approach .....	2
2.2	Evaluation of Nuclear Physics Parameter Covariances .....	3
2.3	Evaluation Sensitivity Coefficients for Integral Experiments.....	3
2.4	Data Assimilation.....	4
3.	$^{23}\text{Na}$ INTEGRAL EXPERIMENT ANALYSIS .....	4
3.1	EURACOS Sodium Neutron Propagation Experiment.....	4
3.2	JANUS-8 Sodium Neutron Propagation Experiment.....	5
4.	$^{23}\text{Na}$ CONSISTENT DATA ASSIMILATION .....	6
5.	$^{56}\text{Fe}$ INTEGRAL EXPERIMENT ANALYSIS .....	9
5.1	Analysis of Ispra Iron Benchmark Experiment (EURACOS) .....	10
5.2	Analysis of ZPR3 Assembly 54 .....	13
6.	$^{56}\text{Fe}$ CONSISTENT DATA ASSIMILATION .....	16
7.	CONCLUSIONS AND FUTURE WORK.....	17
	ACKNOWLEDGMENTS .....	18
	REFERENCES .....	18

## 1. INTRODUCTION

The major drawback of the classical adjustment method is the potential limitation of the domain of application of the adjusted data since adjustments are made on multigroup data, and the multigroup structure, the neutron spectrum used as weighting function and the code used to process the basic data file are significant constraints.

A new approach has been developed in order to adjust physical parameters and not multigroup nuclear data, the objective being now to correlate the uncertainties of some basic parameters that characterize the neutron cross section description, to the discrepancy between calculation and experimental value for a large number of clean, high accuracy integral experiments.

This new approach is the first attempt to build up a link between the wealth of precise integral experiments and basic theory of nuclear reactions. A large amount of exceptionally precise integral measurements has been accumulated over last 50 years. These experiments were driven by the necessities of nuclear applications but were never fully exploited for improving predictive power of nuclear reaction theory. Recent advances in nuclear reaction modeling and neutron transport calculations, combined with sensitivity analyses methods offer a reasonable possibility of de-convoluting results of the integral experiments in a way to obtain feedback on parameters entering nuclear reaction models. Essential ingredients of such a procedure will be covariances for model parameters and sensitivity matrices. The latter will provide direct link between reaction theory and integral experiments. By using integral reactor physics experiments (meter scale), information is propagated back to the nuclear level (femtometers) covering a range of more than 13 orders of magnitude.

The assimilation procedure results in more accurate and more reliable evaluated data files that will be of universal validity rather than tailored to a particular application. These files will naturally come with cross section covariances incorporating both microscopic and integral measurements as well as constraints imposed by the physics of nuclear reactions. Thus, these covariances will encompass the entire relevant knowledge available at the time of evaluation.

On the physics side, the assimilation improves knowledge of model parameters, increasing the predictive power of nuclear reaction theory and it would bring a new quality into nuclear data evaluation as well as refinements in nuclear reaction theory.

## 2. THEORY

The classical “statistical adjustment” techniques [1,2,3] provide adjusted multigroup nuclear data for applications, together with new, improved covariance data and reduced uncertainties for the required design parameters, in order to meet target accuracies.

One should, however, set up a strategy to cope with the drawbacks of the methodology, which are related to the energy group structure and energy weighting functions adopted in the adjustment.

In fact, the classical statistical adjustment method can be improved by “adjusting” reaction model parameters rather than multigroup nuclear data. The objective is to associate uncertainties of certain model parameters (such as those determining neutron resonances, optical model potentials, level densities, strength functions, etc.) and the uncertainties of theoretical nuclear reaction models themselves (such as optical model, compound nucleus, pre-equilibrium and

fission models) with observed discrepancies between calculations and experimental values for a large number of integral experiments. The experiments should be clean (i.e., well documented with high QA standards) and high accuracy (i.e., with as low as possible experimental uncertainties and systematic errors), and carefully selected to provide complementary information on different features and phenomena, e.g., different average neutron spectrum energy, different adjoint flux shapes, different leakage components in the neutron balance, different isotopic mixtures and structural materials etc.

In the past, a few attempts were made [4,5,6] to apply a consistent approach for improving basic nuclear data, in particular to inelastic discrete levels and evaporation temperatures data of  $^{56}\text{Fe}$  for shielding applications, and to resolved resonance parameters of actinides (e.g.,  $\Gamma$  and total widths, peak positions etc.). This effort indicated the validity of the approach but also challenges to be overcome for its practical application. This was mainly related to the way of getting the sensitivity coefficients and to the need of reliable covariance information.

## 2.1 Consistent Data Assimilation Approach

The Consistent Data Assimilation methodology allows overcoming both difficulties, using the approach that involves the following steps:

- Selection of the appropriate reaction mechanisms along with the respective model parameters to reproduce adopted microscopic cross section measurements with the EMPIRE [7] code calculations. Use of coupled channels, quantum-mechanical pre-equilibrium theories, and advanced statistical model accounting for width fluctuations and full gamma cascade ensure state of the art modelling of all relevant reaction mechanisms.
- Determination of covariances matrices for the set of nuclear reaction model parameters obtained in the previous step. This is achieved by combining initial estimates of parameter uncertainties, with uncertainties/covariances for the adopted experimental data through the KALMAN [8] code. This way, the resulting parameter covariances will contain constraints imposed by nuclear reaction theory and microscopic experiments. Several parameters have been considered, including resonance parameters for a few dominating resonances, optical model parameters for neutrons, level density parameters for all nuclei involved in the reaction, parameters entering pre-equilibrium models, and parameters determining gamma-strength functions.
- Sensitivity of cross sections to the perturbation of the above mentioned reaction model parameters are calculated with the EMPIRE code.
- Use of the adjoint technique to evaluate sensitivity coefficients of integral reactor parameters to the cross section variations, as described in the previous step. To perform this task, the ERANOS code system [9] that computes sensitivity coefficients based on generalized perturbation theory is employed.
- Performing analysis of selected experiments using the best calculation tools available (in general Monte Carlo codes like MCNP).
- Performing consistent data assimilation on basic nuclear parameters using integral experiment analysis with best methodology available to provide discrepancies between calculation and measured quantities. After the C/E's are available, they are used together with the sensitivity coefficients coming from the previous step in a data assimilation code.
- Constructing new ENDF/B type data files based on modified reaction theory parameters for use by neutronic designers.

## 2.2 Evaluation of Nuclear Physics Parameter Covariances

As indicated in the outline of the methodology, the first step is to provide estimated range of variation of nuclear physics parameters, including their covariance data. To this end the code EMPIRE [7] coupled to the KALMAN [8] code is employed.

KALMAN code is an implementation of the Kalman filter technique based on minimum variance estimation. It naturally combines covariances of model parameters, of experimental data and of cross sections. This universality is a major advantage of the method. KALMAN uses measurements along with their uncertainties to constrain covariances of the model parameters via the sensitivity matrix. Then, the final cross section covariances can be calculated from the updated covariances for model parameters. This procedure consistently accounts for the experimental uncertainties and the uncertainties of the nuclear physics parameters. We emphasize that under the term 'reaction model' we mean also the resonance region described by models such as the Multi-Level Breit-Wigner formalism.

## 2.3 Evaluation Sensitivity Coefficients for Integral Experiments

In order to evaluate the sensitivity coefficients of the nuclear parameters to the integral parameters measured in a reactor physics experiment, a folding procedure is applied, where the sensitivity calculated by EMPIRE, are folded with those calculated by ERANOS (i.e multigroup cross section sensitivity coefficient to integral parameters).

Following this procedure, the sensitivities of integral experiments to nuclear parameters  $p_k$  are defined as:

$$\frac{\Delta R}{\Delta p_k} = \sum_j \frac{\Delta R}{\Delta \sigma_j} \times \frac{\Delta \sigma_j}{\Delta p_k} \quad (1)$$

where  $R$  is an integral reactor physics parameter (e. g.  $K_{\text{eff}}$ , reaction rates, reactivity coefficient, etc.), and  $\sigma_j$  a multigroup cross section (the  $j$  index accounts for isotope, cross section type and energy group).

In general to compute  $\sigma_j$  one can use a) EMPIRE with an appropriate set of parameters  $p_k$  to generate first b) an ENDF/B file for that specific isotope and successively, c) to use NJOY, to obtain multi-group cross sections.

As specified in the previous section, one can compute the variation of the cross sections  $\Delta \sigma_j$  resulting from a variation of each parameter  $p_k$  variation.

Specifically, the procedure would consist in the generation of the  $\Delta \sigma_j$  corresponding to fixed, well chosen variations of each  $p_k$  taken separately and therefore generating the  $\frac{\Delta \sigma_j}{\Delta p_k}$ . Following

each EMPIRE calculation, an ENDF/B file for the isotope under consideration is generated and a subsequent run of NJOY on this file generates multigroup cross sections in the same energy structure used for the computation of the reactor physics integral parameters. The multigroup cross section variations associated to the individual fundamental parameter that has been varied in the corresponding EMPIRE calculation are readily computed by difference with the reference NJOY calculation for the isotope under consideration.

In parallel, the cross section sensitivity coefficients to integral parameter  $R$ :



$$\frac{\Delta R}{\Delta \sigma_j}$$

are provided, using the standard Generalized Perturbation Theory in the ERANOS code system.

Folding the two contributions (from EMPIRE and ERANOS) one obtains the sensitivity coefficients of the nuclear physics parameters to the integral measured parameters, see Eq. (1).

## 2.4 Data Assimilation

Finally as far as data adjustment (or data “assimilation”) the methodology makes use of:

- quantified uncertainties and associated variance-covariance data;
- well documented, high accuracy and “representative” integral experiments;
- sensitivity coefficients for a variety of integral parameters.

A statistical adjustment is performed using these quantities. Formulation is given in reference [1].

As a practical example we have considered the case of two structural isotopes:  $^{23}\text{Na}$  and  $^{56}\text{Fe}$ .

## 3. $^{23}\text{Na}$ INTEGRAL EXPERIMENT ANALYSIS

For this case we have used propagation experiments of neutrons in a medium dominated by this specific isotope. These kinds of experiments were specifically intended for improving the data used in the shielding design of fast reactors. Two experimental campaigns taken from the SINBAD database [10] have been used in this practical application: the EURACOS campaign, and the JANUS-8 campaign.

### 3.1 EURACOS Sodium Neutron Propagation Experiment

The Ispra sodium benchmark project was performed under the EURACOS (Enriched URanium CONverter Source) irradiation facility. The main purpose of this experiment was to study the neutron deep penetration in homogeneous materials found in the construction of advanced reactors (i.e., Na and Fe). Thus, the analysis of this experiment can be effectively utilized for the sodium cross section improvement. The neutron source of this system is made by the Al-U plate, having 80 cm in diameter and 1.8 cm in thickness. This source is driven by TRIGA Mark II reactor located right next to this irradiation facility. Measurements with activation detectors were carried out at distances from the source 18.35, 66.4, 125.2, 184.5, 243.2, 302.4, 362.2 cm for  $^{32}\text{S}(\text{n},\text{p})$  and  $^{197}\text{Au}(\text{n},\gamma)$  in order to analyze fast and epithermal neutron attenuations.

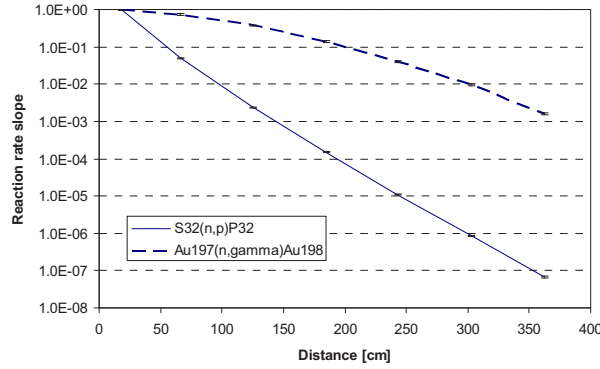


**Fig.1.** Neutron attenuation of EURACOS sodium experiment for  $^{32}\text{S}$  and  $^{197}\text{Au}$  detectors. (Error bars =  $\pm 1\sigma$ )

Analysis was performed by the Monte Carlo code MCNP5 using the  $^{23}\text{Na}$  data of ENDF/B-VII and those coming directly from EMPIRE (see reference [11]).

The EMPIRE cross sections are quite consistent with those of ENDF/B-VII and in some case are performing better. The calculated attenuations for the two detectors are shown in Fig.1 (slopes are normalized to the first position of measured detector).

### 3.2 JANUS-8 Sodium Neutron Propagation Experiment

The JANUS Phase 8 experiments were performed at the ASPIS facility. The neutron source was generated by Al-U plate, which is driven by the NESTOR reactor, a 30kW light water cooled, graphite and light water moderated reactor, located right next to this experimental facility. The distance between this source plate and the last detector point is approximately 300 cm. A  $\sim 18$  cm thick zone of mild steel plates precedes the sodium tanks.

Again the computational analysis was carried out with MCNP5 with EMPIRE cross section data. The neutron attenuations of several different detectors were analyzed and in particular for the following reaction rates:  $^{32}\text{S}(n,p)^{32}\text{P}$ ,  $^{103}\text{Rh}(n,n')^{103\text{m}}\text{Rh}$ ,  $^{197}\text{Au}(n,\gamma)^{198}\text{Au}$ , and  $^{55}\text{Mn}(n,\gamma)^{56}\text{Mn}$ . Fig. 2 shows the attenuations obtained for the different sets of detector reaction rate slopes normalized at the first measured position.

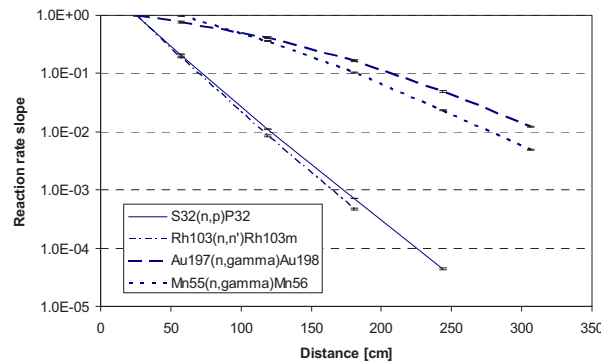


**Fig. 2.** Neutron attenuation of JANUS-8 sodium experiment for  $^{32}\text{S}$ ,  $^{197}\text{Au}$ ,  $^{55}\text{Mn}$ , and  $^{103}\text{Rh}$  detectors. (Error bars =  $\pm 1\sigma$ )

#### 4. $^{23}\text{Na}$ CONSISTENT DATA ASSIMILATION

In order to perform the consistent data assimilation on the  $^{23}\text{Na}$  a set of 136 nuclear parameters were selected and sensitivities to them in terms of multigroup cross section were calculated (Ref. [11] provides the details of this step). The selected parameters include: scattering radius, bound level and 33 resonances (for each one:  $E_n$  resonance peak energy,  $\Gamma_n$  neutron width,  $\Gamma_g$  radiative width, for a total of 102 parameters), 33 parameters in fast region (21 Optical model parameters, 7 Statistical Hauser-Feshbach model parameters, and 5 Preequilibrium Exciton model parameters).

For what concerns the experiments, a set of reaction rate slopes (one for each detector in the two experiment campaigns) was selected. The selection was based, on: low experimental and calculation uncertainty, good depiction of the neutron attenuation for the energy range to be characterized by the corresponding detector, complement of information (obtained by correlation calculations using the sensitivity coefficients), and good consistency among the C/E on the selected slopes. The selected slopes were the ratios of the fourth position to the first one for both detectors in the EURACOS experiment, while for the JANUS-8 experiment we selected the fourth to first position ratio for the  $^{32}\text{S}$  and  $^{197}\text{Au}$  detectors, fourth to second position for the  $^{55}\text{Mn}$  (there was no measurement in the first position), and third to first for the  $^{103}\text{Rh}$  (the fourth position has a very large experimental uncertainty).

**Table 1** C/E of the selected slopes

Detector	C/E
EURACOS $^{32}\text{S}$	<b><math>0.770 \pm 0.085</math></b>
EURACOS $^{197}\text{Au}$	<b><math>0.954 \pm 0.102</math></b>
JANUS-8 $^{32}\text{S}$	<b><math>0.538 \pm 0.022</math></b>
JANUS-8 $^{197}\text{Au}$	<b><math>1.010 \pm 0.033</math></b>
JANUS-8 $^{55}\text{Mn}$	<b><math>1.158 \pm 0.025</math></b>
JANUS-8 $^{103}\text{Rh}$	<b><math>0.960 \pm 0.106</math></b>

A 41 group energy structure was adopted specifically to better describe the resonance structure of the  $^{23}\text{Na}$ . The ERANOS code was used to calculate the multigroup sensitivity for the selected reaction rate slopes.

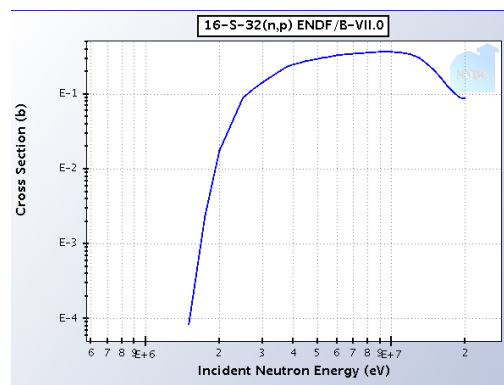


**Fig. 3.**  $^{32}\text{S}(\text{n,p})$  point energy cross section.

In order to better understand the choice of the selected slopes and their related C/E, in Table 2 we show the sensitivity coefficients to elastic and inelastic cross sections for the  $^{32}\text{S}$  detector in

both EURACOS and JANUS-8. As it can be seen there are some large differences between the two experiments. The <sup>32</sup>S(n,p) reaction is a threshold reaction (see Fig. 3) and because of the presence of the mild steel zone in JANUS-8 a quite different (softer) neutron spectrum is present at the starting point of measurement, which produces both the different C/E and sensitivities between the two experiments.

Table 3 illustrates the correlation factors among the different detector reaction rate slopes in the two experiments. These correlation factors are calculated using the sensitivity coefficients and covariance matrix used later in the adjustment step [12]. In fact the following equation is used:

$$Corr_{12} = \frac{S_1 D S_2^+}{[(S_1 D S_1^+)(S_2 D S_2^+)]^{1/2}}$$

where  $Corr_{12}$  is the correlation factor between experiment 1 and 2,  $S_1$  and  $S_2$  the sensitivity coefficient arrays for experiment 1 and 2, and  $D$  the covariance matrix

**Table 2** <sup>32</sup>S sensitivity coefficients.

Upper Energy (Mev)	Sensit. $\sigma^{\text{elastic}}$ EUR.	Sensit. $\sigma^{\text{elastic}}$ JANUS	Sensit. $\sigma^{\text{incl.}}$ EUR.	Sensit. $\sigma^{\text{incl.}}$ JANUS
19.64	-7.3 10 <sup>-3</sup>	-4.5 10 <sup>-2</sup>	-4.8 10 <sup>-2</sup>	-1.6 10 <sup>-1</sup>
10.00	-1.3 10 <sup>-1</sup>	-2.1 10 <sup>-1</sup>	-6.6 10 <sup>-1</sup>	-9.9 10 <sup>-1</sup>
6.065	-8.4 10 <sup>-1</sup>	-1.4	-1.9	-2.9
3.678	-9.0 10 <sup>-1</sup>	-4.0	-1.1	-2.8
2.231	-2.9 10 <sup>-1</sup>	-2.4	-1.8 10 <sup>-1</sup>	-8.6 10 <sup>-1</sup>

**Table 3** Correlations among experiments.

	<sup>32</sup> S EUR.	<sup>19</sup> <sup>7</sup> Au EUR.	<sup>32</sup> S JAN.	<sup>19</sup> <sup>7</sup> Au JAN.	<sup>55</sup> Mn JAN.	<sup>10</sup> <sup>3</sup> Rh JAN.
<sup>32</sup> S EUR.	1	-	0	0	0	0
<sup>19</sup> <sup>7</sup> Au EUR.	.00	1	.08	0	.00	.02
<sup>32</sup> S JAN.	.00	.04	1	0	.00	.04
<sup>19</sup> <sup>7</sup> Au JAN.	.13	.00	.04	1	.31	0.16
<sup>55</sup> Mn JAN.	.08	.04	.00	.00	1	.28
<sup>10</sup> <sup>3</sup> Rh JAN.	.02	.29	.04	0.16	.28	1

JAN. <sup>10</sup>						
<sup>3</sup> Rh	0	-	0	-	0	1
JAN.	.02	0.29	.04	0.16	.28	.00

As it can be observed there is relatively little correlation among the selected slopes insuring, in this way, a good complementarity of information to be exploited in the data assimilation step.

A specific code was written in order to manipulate the two sets of sensitivities (nuclear parameters, and integral experiments to multigroup cross sections) check their consistency, calculate uncertainties on measured parameters, and perform the folding of Eq. (1).

Once obtained the sensitivity of nuclear parameters to the integral experiments, they were used together with the C/E of the computational analysis shown in Section 3 for a statistical adjustment. Table 4 shows the C/E after the adjustments for the selected reaction rates slopes.

As it can be observed, except for the gold detectors that did already show good C/E agreement, a remarkable improvement is obtained after the adjustments.

The corresponding variations of the nuclear parameters that are needed for obtaining such improvement are shown in Table 5. Only the parameters that require at least 0.3% of variation are reported, and for the meaning of the parameter name we refer to [11].

**Table 4** C/E after statistical adjustment

Detector	C/E after adj.
EURACOS <sup>32</sup> S	<b>0.997 ± 0.057</b>
EURACOS <sup>197</sup> Au	<b>0.946 ± 0.010</b>
JANUS-8 <sup>32</sup> S	<b>1.000 ± 0.022</b>
JANUS-8 <sup>197</sup> Au	<b>0.959 ± 0.028</b>
JANUS-8 <sup>55</sup> Mn	<b>1.028 ± 0.023</b>
JANUS-8 <sup>103</sup> Rh	<b>0.976 ± 0.047</b>

All the variations are in less than  $1\sigma$  of the initial uncertainties and, therefore, look acceptable. Some important parameters show a significant improvement in the “a posteriori” standard deviation (e.g. scattering radius) that would translate in reduced uncertainties on design parameters when the “assimilated” cross sections will be used. The only concern regards to the  $\Gamma_n$  of the resonance at 538 Kev that requires a very large variation almost corresponding to the initial standard deviation. More investigation is needed in order to see if this kind of variation is realistic.

**Table 5** Parameter variations and standard deviations obtained by data assimilation.

Parameter	Variation (%)	Init. Stand. Dev. (%)	Final Stand. Dev. (%)
Scat. Rad. <sup>a)</sup>	<b>1.9</b>	<b>4.1</b>	<b>1.7</b>
$\Gamma_n$ Bou. Lev. <sup>b)</sup>	<b>-6.4</b>	<b>8.0</b>	<b>6.4</b>
$\Gamma_n$ 2.8 Kev <sup>c)</sup>	<b>0.6</b>	<b>1.9</b>	<b>1.9</b>
$\Gamma_g$ 2.8 Kev <sup>c)</sup>	<b>10.5</b>	<b>11.8</b>	<b>10.5</b>
$\Gamma_n$ 538 Kev <sup>c)</sup>	<b>-57.2</b>	<b>65.9</b>	<b>58.4</b>
R. Vol. Rad. <sup>d)</sup>	<b>-1.8</b>	<b>2.8</b>	<b>1.6</b>
R. Surf. Dif. <sup>e)</sup>	<b>-0.8</b>	<b>5.0</b>	<b>4.7</b>
R. Vol. Dif. <sup>f)</sup>	<b>-0.4</b>	<b>2.1</b>	<b>2.1</b>
TOTRED <sup>g)</sup>	<b>-1.1</b>	<b>3.5</b>	<b>3.2</b>
FUSRED <sup>h)</sup>	<b>-0.8</b>	<b>5.0</b>	<b>4.0</b>

- <sup>a)</sup> Nuclear Scattering Radius, <sup>b)</sup> Bound Level resonance, <sup>c)</sup> Resonance Peak Energy  
<sup>d)</sup> Optical model real volume radius for target nucleus, <sup>e)</sup> Optical model real surface diffuseness for target nucleus, <sup>f)</sup> Optical model real volume diffuseness for target nucleus  
<sup>g)</sup> Optical model scaling of total cross sections due to intrinsic model uncertainty  
<sup>h)</sup> Optical model scaling of absorption cross sections due to intrinsic model uncertainty

In order to appreciate the impact of these variations we show in Table 6 and 7 their contribution to the relative change of the C/E for the case of two detectors.

As it can be seen the improved C/E is the result of very large compensations after the parameters have been adjusted. Of special interest are the results of Table 5 regarding the two slopes of  $^{32}\text{S}$ . One can appreciate how the assimilated new parameters are able to compensate and adjust the two C/E that were large and quite different.

**Table 6** Contribution of the parameter variation to the relative change of the C/E of the  $^{32}\text{S}$  slopes of EURACOS and JANUS-8

Parameter	EURACOS Contrib. (%)	JANUS-8 Contrib. (%)
R. Vol. Rad.	<b>20.2</b>	<b>61.6</b>
TOTRED	<b>3.9</b>	<b>13.4</b>
FUSRED	<b>2.0</b>	<b>2.9</b>
R. Surf. Dif	<b>1.7</b>	<b>5.2</b>
R. Vol. Dif.	<b>1.9</b>	<b>3.3</b>
Total	<b>29.5</b>	<b>85.8</b>

**Table 7** Contribution of the parameter variation to the relative change of the C/E of the  $^{55}\text{Mn}$  slope of JANUS-8

Parameter	Contribution (%)
Scat. Rad.	<b>-12.4</b>
$\Gamma_n$ Bou. Lev.	<b>8.0</b>
$\Gamma_g$ 2.8 Kev	<b>4.4</b>
$\Gamma_n$ 538 Kev	<b>-2.6</b>
R. Vol. Rad.	<b>1.0</b>
$\Gamma_g$ 2.8 Kev	<b>-1.3</b>
Total	<b>-11.2</b>

The  $\chi^2$  test after adjustment provided a value of 5.95, which is quite good in view of the fact that, for the statistical adjustment methodology adopted, the degrees of freedom of the problem are that of the number of experiments used in the adjustment, in this case 6.

## 5. $^{56}\text{Fe}$ INTEGRAL EXPERIMENT ANALYSIS

For the  $^{56}\text{Fe}$  data assimilation two classes of experimental programs were considered. One, as in the case of  $^{23}\text{Na}$ , is of the type of propagation experiment, where the attenuation of the neutron propagation is dictated by the main structural isotope. The other is of the reflector interface effect type [13], where a spectrum transient between a reactor core and its surrounding is dominated by the presence of an iron reflector.

## 5.1 Analysis of Ispra Iron Benchmark Experiment (EURACOS)

As we have selected for the  $^{23}\text{Na}$  data assimilation, Ispra benchmark experiment (EURACOS) [10] also has a set of reliable measurements for the neutron deep penetration through homogeneous iron slabs. The EURACOS II facility consists of blocks of iron slabs having dimensions approximately  $145 \times 145 \times 130 \text{ cm}^3$  surrounded by thick concrete walls. The neutron source is made by U-Al alloy circular disc source having a diameter of 80 cm and a thickness of 1.8 cm. This disc source is driven by thermal neutrons from 250 kW TRIGA MARK II reactor located right next to this facility. A Boral plate is placed between the source and the Fe block to reduce the low energy neutrons from the TRIGA reactor. A Boral plate is placed between the source and the Fe block to reduce the low energy neutrons from the TRIGA reactor.

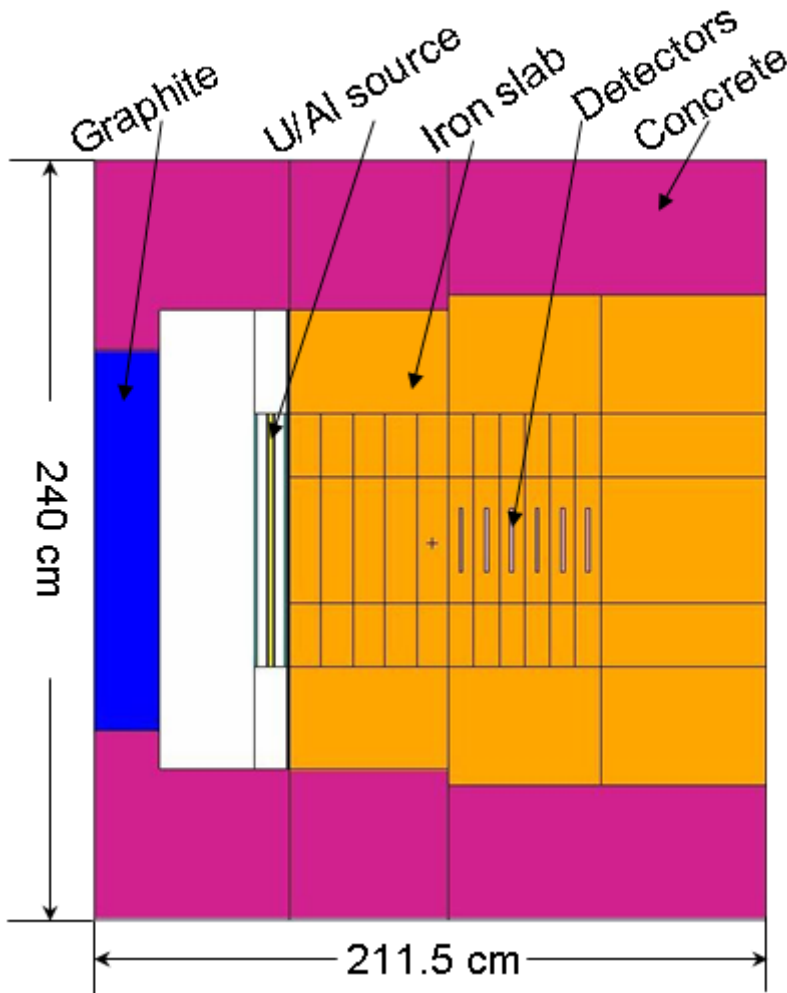


Figure 4: MCNP model of EURACOS iron experiment

The EURACOS system for iron benchmark was modeled for both MCNP5 and ERANOS [9] calculations. This irradiation facility was almost explicitly modeled for MCNP5. This model is shown in Figure 4. For the MCNP5 calculations, in order to obtain statistically reliable reaction rates at each detector point, the variance reduction technique via weight windows was utilized. All detectors were modeled according to detector compositions shown in Reference 10, except for the first 7 detectors for  $\text{S32}(n,p)\text{P32}$  reaction rate calculations since dimensions of those detectors were negligibly small. For the ERANOS deterministic calculations, the MCNP model

was equivalently transformed into the 2-dimensional cylindrical geometry (R-Z). The calculations were performed with 84043 spatial meshes,  $S_4$  quadratures, and  $P_1$  scattering expansion. The 33-group cross sections of each material zone and fission spectrum of the U-Al plate were prepared by ECCO lattice physics code. None of detectors were modeled explicitly. MCNP5 calculations were performed with  $^{56}\text{Fe}$  cross sections from both ENDF/B-VII and EMPIRE [7] calculations. Only ENDF/B-VII library was used for ERANOS calculations.

Figures 5 through 8 show the comparisons of  $\text{S32}(n,p)\text{P32}$ ,  $\text{Au197}(n,\gamma)\text{Au198}$ ,  $\text{In115}(n,n')$ , and  $\text{Rh103}(n,n')$  reaction rate slopes, respectively, obtained by MCNP5 and ERANOS calculations. As seen in these plots, all calculated results near the first detector location generally agrees well, and the magnitude of discrepancy from the experimental results propagates as the detector location becomes far from the first one. This is the expected phenomenon since the reaction rate slopes were taken respect to the result of the first detector. Comparing the results obtained based on ENDF/B-VII, the C/E's of MCNP5 and ERANOS results have almost similar quality. The C/E of MCNP5 results based on EMPIRE  $\text{Fe}^{56}$  cross sections shows different behavior from those obtained with ENDF/B-VII, in particular for the  $\text{In115}(n,n')$  and  $\text{Rh103}(n,n')$  reaction rate slopes; however, overall the ENDF/B-VII cross sections slightly outperforms the EMPIRE ones.

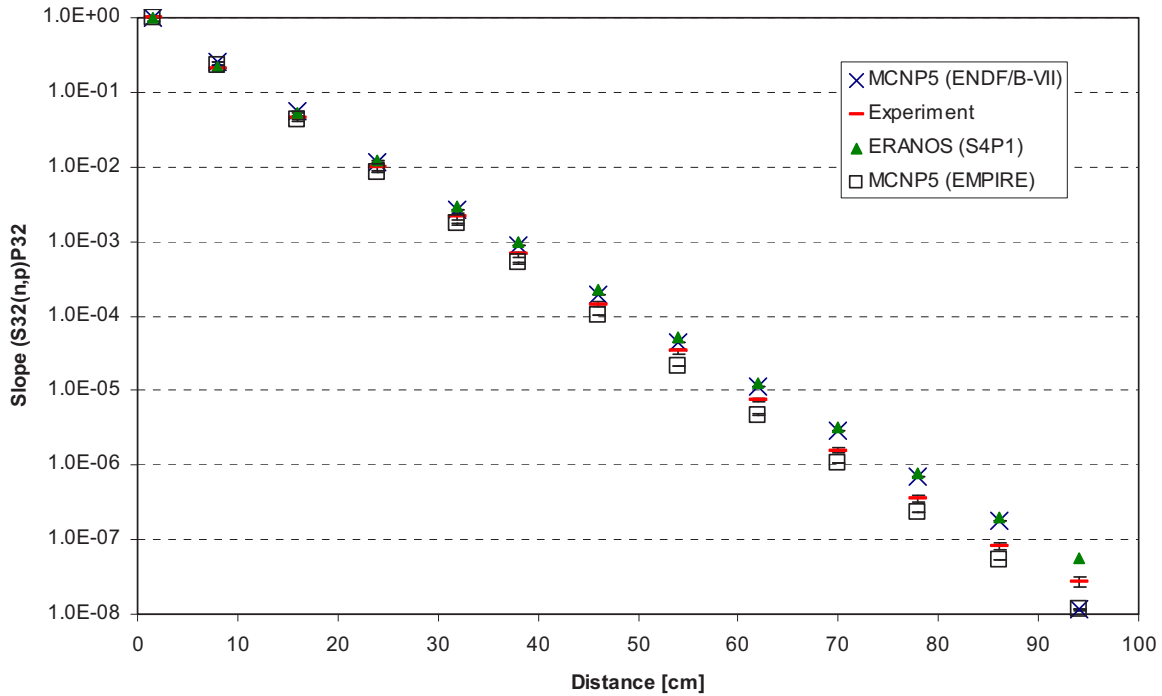
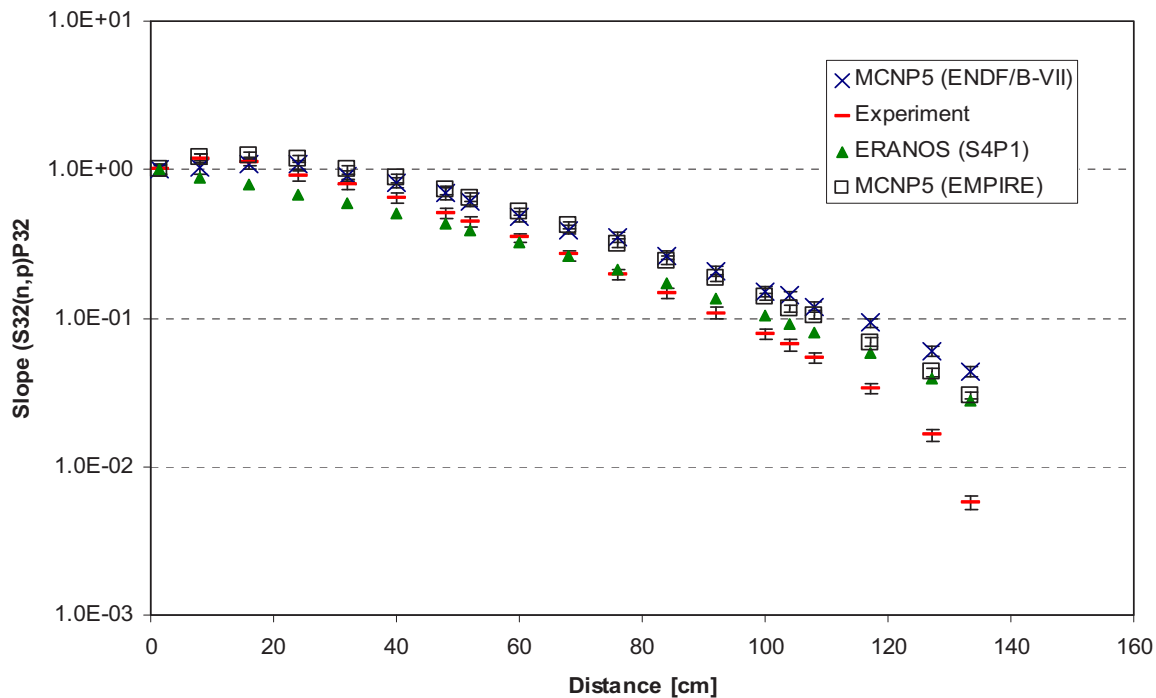
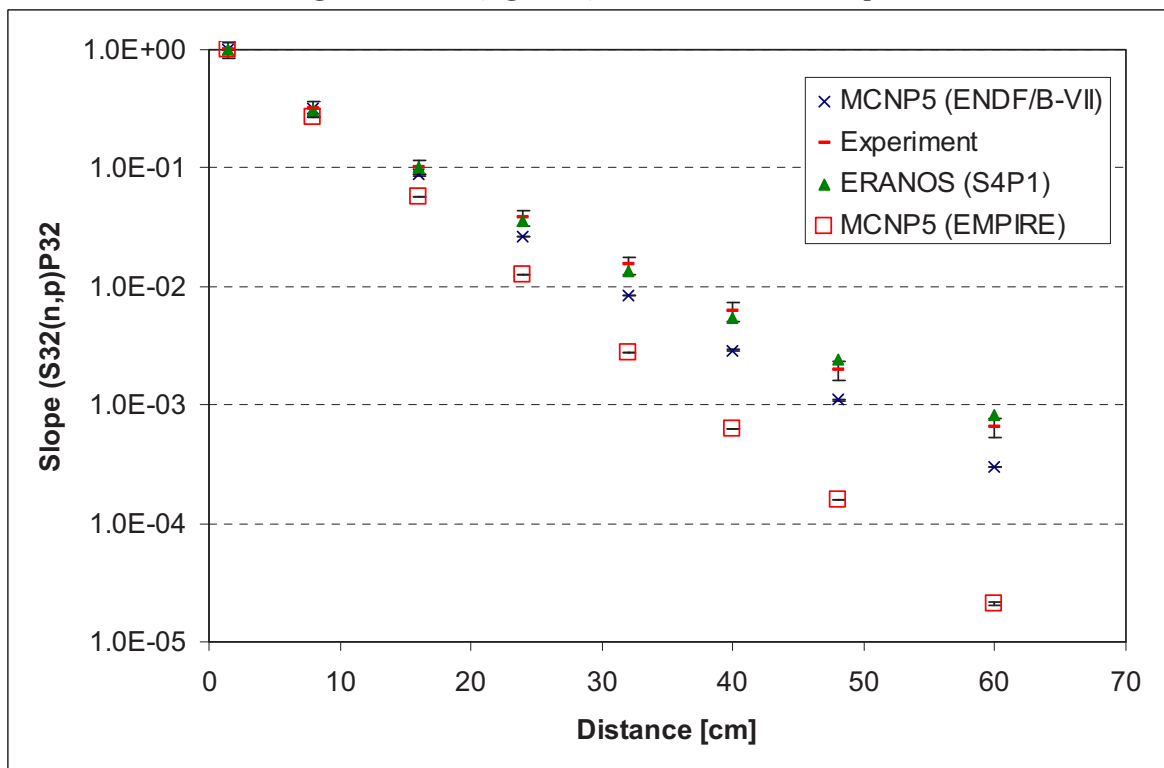


Figure 5:  $\text{S32}(n,p)\text{P32}$  reaction rate slope.



Figure 6:  $\text{Au197}(n,\gamma)\text{Au198}$  reaction rate slope.Figure 7:  $\text{In115}(n,n')\text{In115}$  reaction rate slope.

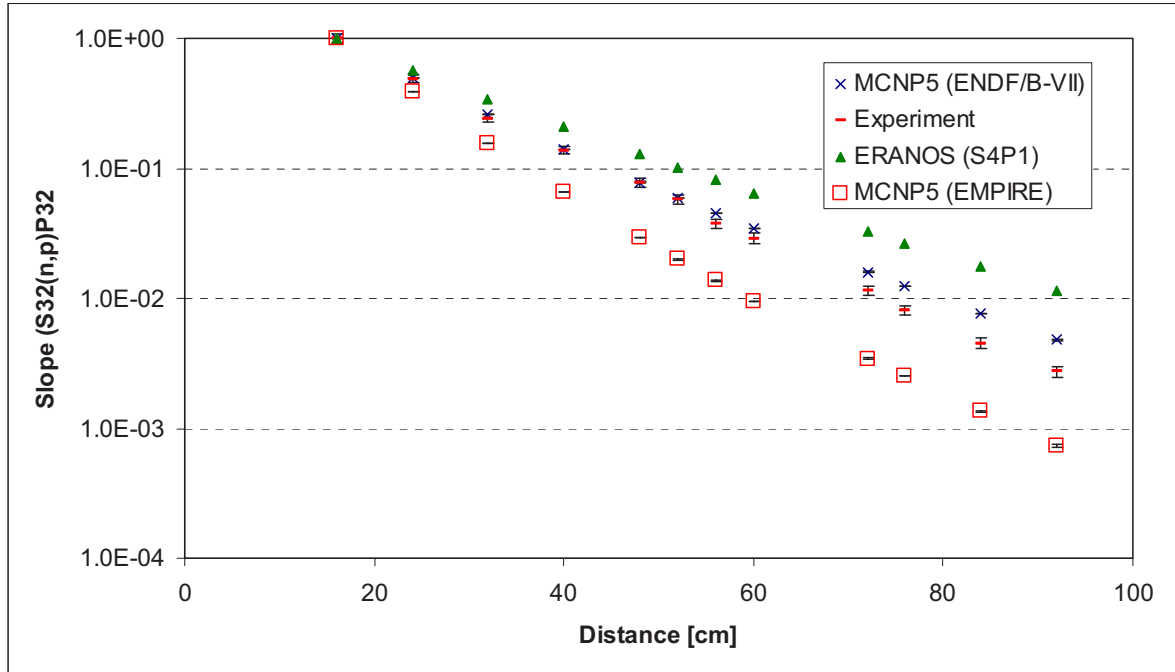


Figure 8: Rh103 (n,n') reaction rate slope.

## 5.2 Analysis of ZPR3 Assembly 54

ZPR3 54 assembly has a Plutonium-fueled cylindrical core of 24 inch long and about 27 and 25.2 inch in diameter, respectively with a large presence of carbon. Assembly 53 is surrounded by a 12-inch-thick blanket both radially and axially while this blanket is replaced with a mild steel reflector in Assembly 54. The analyses of these assemblies were performed using both detailed and homogenized (cylindrical) models. These models were made based on the descriptions of detailed drawer configurations and material number densities given in [14].

The benchmark models used for  $k_{eff}$  calculations were modified to perform calculations for radial reaction rate traverses. For the detailed model, reaction rates were tallied by positioning the small cylindrical chamber with sensitive materials ( $^{239}\text{Pu}$ ,  $^{238}\text{U}$ ,  $^{235}\text{U}$ , and  $^{10}\text{B}$ ) in a stainless steel guide tube (see Figure 9). The steel guide tube is located in the fixed half of the assembly with its axis 1 in. back from the interface. For the cylindrical model, reaction rates were calculated by multiplying the cross section of interest to the flux tallied at the cylindrical tube zones which have exactly the same size and location as that of detector chamber in the detailed model (see Figure 10).

Reaction rate figures comparison are shown in figures 11 through 14 for the  $^{235}\text{U}(n,f)$ ,  $^{238}\text{U}(n,f)$ ,  $^{239}\text{Pu}(n,f)$ , and  $^{10}\text{B}(n,\alpha)$  detectors. As for the previous cases both ENDF/B-VII and EMPIRE  $^{56}\text{Fe}$  were used. In general as for the EURACOS experiments ENDF/B-VII results outperform those of EMPIRE.

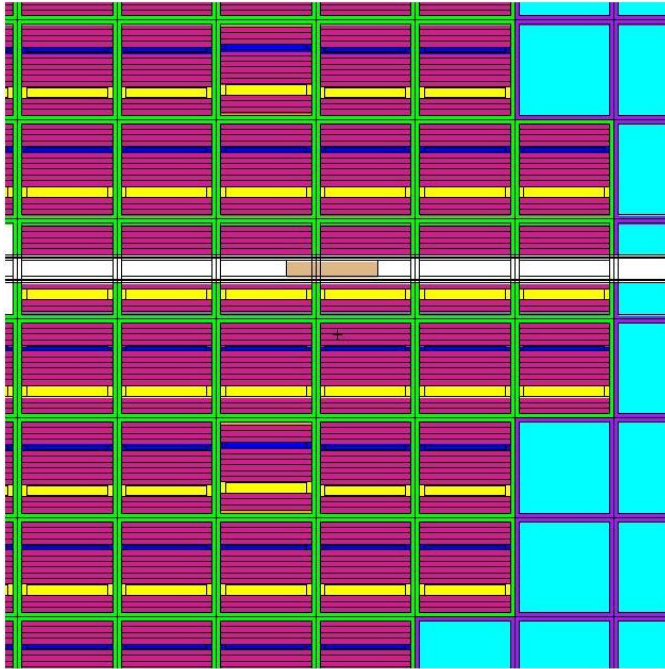


Figure 9. Detector in the heterogeneous model

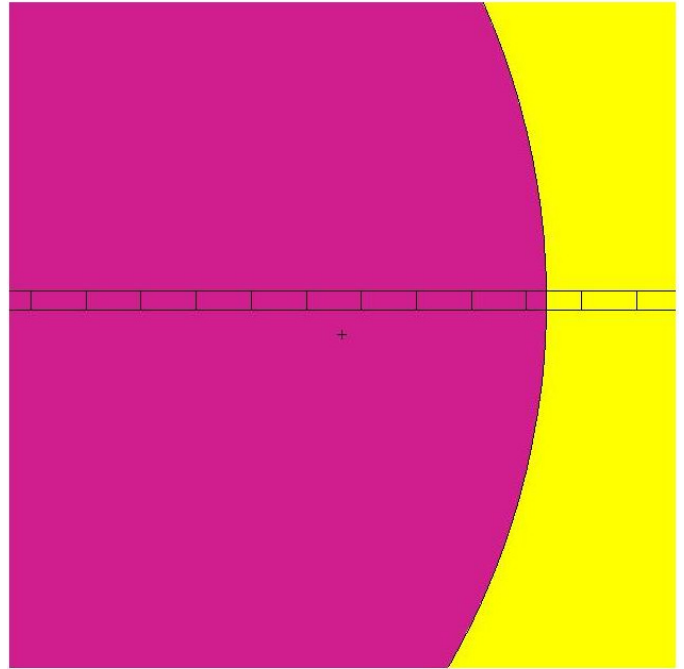


Figure 10. Detector in the cylindrical model.

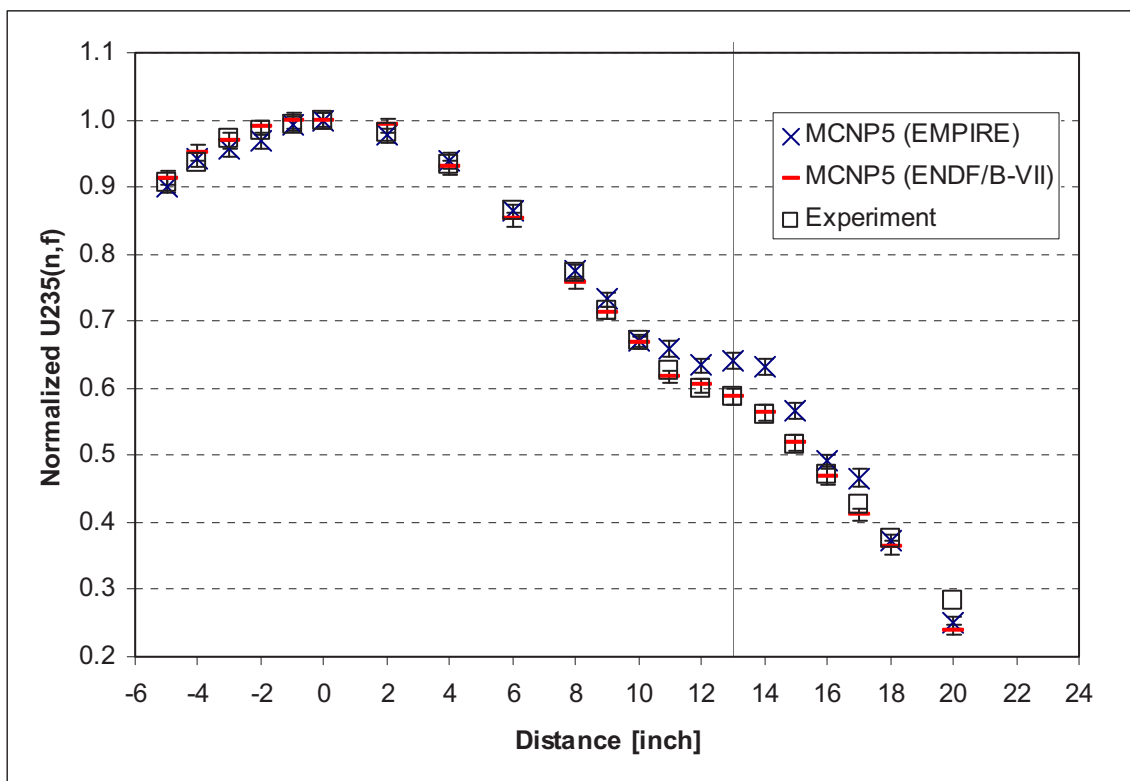


Fig. 11. ZPR3-54 U235 (n,f) reaction rate distributions.

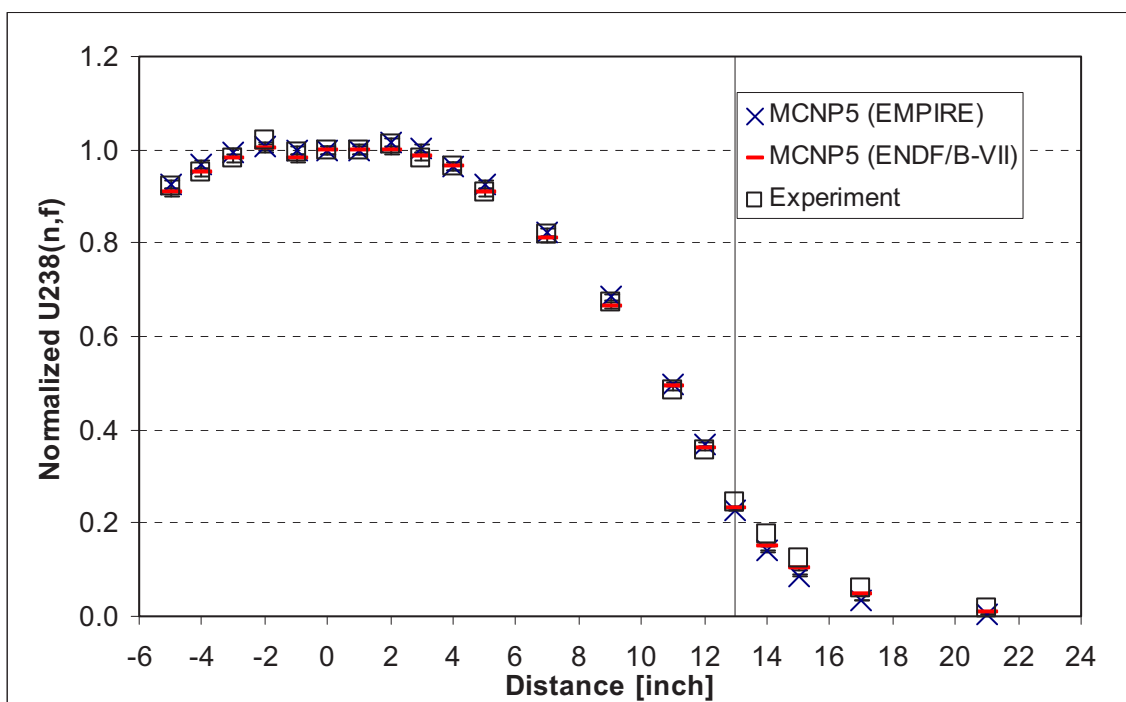


Fig. 12 ZPR3-54 U238 (n,f) reaction rate distributions.

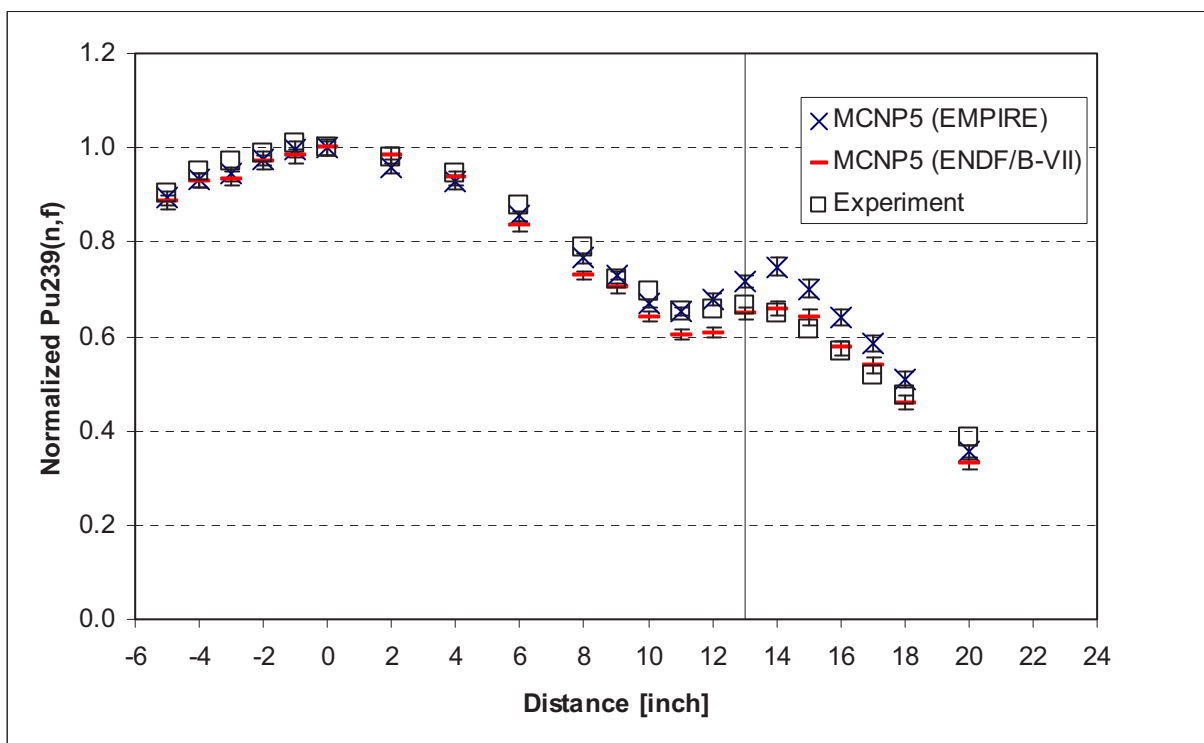
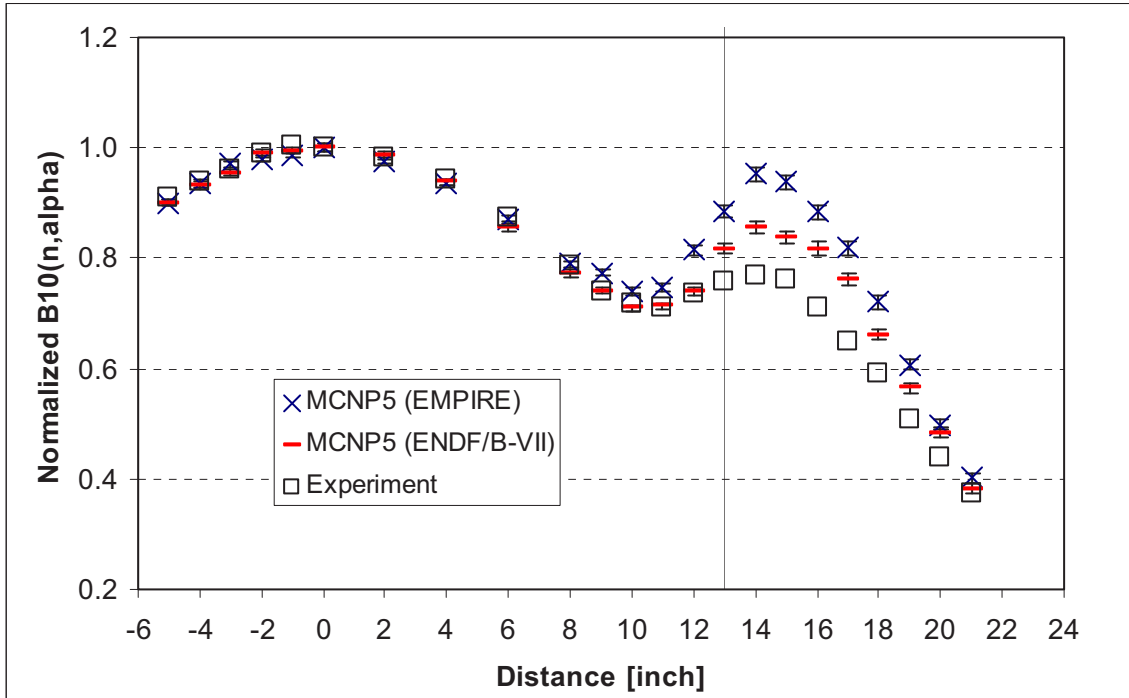


Fig. 13. ZPR3-54 Pu239 (n,f) reaction rate distributions.

Fig. ZPR3-54 B10 (n,  $\alpha$ ) reaction rate distributions

## 6. $^{56}\text{Fe}$ CONSISTENT DATA ASSIMILATION

As in the case of  $^{23}\text{Na}$  a set of nuclear parameters was selected and sensitivities were calculated for the different experimental quantities to be used in the data assimilation process.

This data assimilation for  $^{56}\text{Fe}$  has to be considered very preliminary as one can observe, based on the obtained C/E, the EMPIRE generated  $^{56}\text{Fe}$  appears to be of lower quality when compared to the original ENDF/B-VII data set for this isotope. A total of 35 nuclear parameters were used including: the nuclear radius, nine optical model parameters, peak energy  $\Gamma_n$  and  $\Gamma_g$  for the bound level, and  $\Gamma_n$  for 25 S wave resonances.

For each experimental detector a specific slope, based on consideration of energy spectrum representativity, was selected so that in total 8 experimental values were used in the data assimilation. Table 8 shows the C/E before and after data assimilation.

Table 8. Initial and new C/E before and after data assimilation.

Experiment	old C/E $\pm \sigma$	new C/E $\pm \sigma$	Experiment	old C/E $\pm \sigma$	new C/E $\pm \sigma$
B10(n, $\alpha$ ) Slope ZPR3-54	$0.853 \pm 0.030$	$1.012 \pm 0.022$	S32(n,p) Slope EURACOS	$0.879 \pm 0.093$	$1.197 \pm 0.055$
U235 Fission Slope ZPR3-54	$0.907 \pm 0.030$	$1.015 \pm 0.013$	Au197(n, $\gamma$ ) Slope EURACOS	$1.288 \pm 0.098$	$1.054 \pm 0.032$
Pu239 Fission Slope ZPR3-54	$0.889 \pm 0.030$	$0.996 \pm 0.013$	In115(n,n') Slope EURACOS	$0.327 \pm 0.156$	$0.455 \pm 0.042$
U238 fission Slope ZPR3-54	$1.455 \pm 0.030$	$1.284 \pm 0.014$	Rh103(n,n') Slope EURACOS	$0.478 \pm 0.071$	$0.511 \pm 0.010$

One can observe some significant improvements in the C/E's after assimilation; however,

especially for the slopes in the EURACOS, some of the C/E's stay unacceptable. In table 9 the modifications required for the most important contributors of the used nuclear parameters are shown along their initial and final standard deviations.

Significant reduction in the final standard deviation is observed only for the nuclear scattering radius; however, many parameters show required modifications that are very large (more than  $2\sigma$ ) when compared with the initial standard deviation. This fact combined with the previous observed inability to significantly improve some of the C/E's result in a value of the  $\chi^2$  test (more than 50 times the total degrees of freedom) that is unacceptable.

Likely, some inconsistencies can exist among the experimental values that have been used, or the adopted initial uncertainties for the nuclear parameters are not sufficiently large to cover the observed discrepancies between experimental and calculated values. Moreover, the fact that the  $^{56}\text{Fe}$  generated by EMPIRE performs significantly worse than the existing ENDF/B-VII data set indicates that improvements are needed in the nuclear parameters input to EMPIRE. In conclusion more investigation is needed on the subject and definitely a better data assimilation needs to be performed for  $^{56}\text{Fe}$ .

**Table 9** Parameter variations and standard deviations obtained by data assimilation.

Parameter	Variation (%)	Init. Stand. Dev. (%)	Final Stand. Dev. (%)
Scat. Rad. <sup>a)</sup>	<b>-13.25</b>	<b>5.1</b>	<b>2.1</b>
$\Gamma_n$ Bou. Lev. <sup>b)</sup>	<b>1.9</b>	<b>4.0</b>	<b>3.7</b>
$\Gamma_g$ Bou. Lev. <sup>b)</sup>	<b>-2.1</b>	<b>5.0</b>	<b>4.8</b>
$\Gamma_n$ 277 Kev <sup>c)</sup>	<b>-1.1</b>	<b>8.0</b>	<b>8.0</b>
$\Gamma_n$ 317 Kev <sup>c)</sup>	<b>-2.2</b>	<b>8.0</b>	<b>8.0</b>
$\Gamma_n$ 361 Kev <sup>c)</sup>	<b>-2.9</b>	<b>8.0</b>	<b>8.0</b>
$\Gamma_n$ 381 Kev <sup>c)</sup>	<b>-3.0</b>	<b>8.0</b>	<b>8.0</b>
$\Gamma_n$ 665.6 Kev <sup>c)</sup>	<b>1.3</b>	<b>8.0</b>	<b>8.0</b>
R. Well. Vol. <sup>d)</sup>	<b>15.1</b>	<b>3.0</b>	<b>2.2</b>
Nuc. Rad. R. Surf. <sup>e)</sup>	<b>10.5</b>	<b>3.0</b>	<b>2.9</b>
Im. R. Surf. <sup>f)</sup>	<b>10.8</b>	<b>5.0</b>	<b>4.9</b>
TOTRED <sup>g)</sup>	<b>-0.9</b>	<b>1.0</b>	<b>1.0</b>
FUSRED <sup>h)</sup>	<b>-2.0</b>	<b>1.3</b>	<b>1.2</b>

<sup>a)</sup> Nuclear Scattering Radius, <sup>b)</sup> Bound Level resonance, <sup>c)</sup> Resonance Peak Energy

<sup>d)</sup> Optical model real well depth and real volume of target nucleus, <sup>e)</sup> Optical model nuclear radius and real surface of target nucleus, <sup>f)</sup> Optical model imaginary and real surface of target nucleus, <sup>g)</sup> Optical model scaling of total cross sections due to intrinsic model uncertainty,

<sup>h)</sup> Optical model scaling of absorption cross sections due to intrinsic model uncertainty

## 7. CONCLUSIONS AND FUTURE WORK

We have proposed and implemented a new approach to link integral experiment results to basic nuclear parameters used by evaluators for generating point cross section data files. In this way the improvement in cross sections obtained by data assimilation can be general and not linked to a specific energy group structure as done in the past.

A practical application employing experimental results of neutron propagation in sodium has shown that "adjustments" in a few nuclear parameters of  $^{23}\text{Na}$  can produce remarkable improvements in the agreement between calculation and experiments. The same applications to the  $^{56}\text{Fe}$  case has shown that some inconsistencies exist for this isotope so that more

investigation is needed and further data assimilation will be performed in the next future.

Next steps will involve the use of the modified “adjusted” parameters in EMPIRE to generate ENDF/B type of files that will be used to generate (via NJOY) multigroup data. These multigroup cross sections will be checked against those obtained by a multigroup adjustment where the same experiments used in the consistent data assimilation will be applied.

Furthermore, the consistent data assimilation will be extended to other isotopes.

## ACKNOWLEDGMENTS

The work performed and reported in this document is supported by a project funded by the DOE Office of Science in the framework of the Recovery Act (ARRA).

## REFERENCES

- [1] A. Gandini, M. Petilli, “AMARA: A Code Using the Lagrange Multipliers Methods of Nuclear Data Adjustment,” RT/FI(73)39, Comitato Nazionale per l’Energia Nucleare, Italy (1973).
- [2] A. Gandini, “Uncertainty Analysis and Experimental Data Transposition Methods in Uncertainty Analysis,” Y. Ronen, Editor, CRC Press, 1988.
- [3] M. Salvatores, G. Aliberti, G. Palmiotti, “Nuclear Data Validation and Fast Reactor Design Performances Uncertainty Reduction,” Trans. ANS Meeting, **96**, 519, Boston, Massachusetts, June 22-26, 2007.
- [4] A. Gandini, M. Salvatores, “Nuclear data and Integral Measurements Correlation for Fast reactors-Part 3: The Consistent Method”, RT/FI(74)3, Comitato per l’Energia Nucleare (1974)
- [5] A. D’Angelo, A. Oliva, G. Palmiotti, M. Salvatores, and S. Zero, “Consistent Utilization of Shielding Benchmark Experiments,” *Nuclear Science Engineering* **65**, 477 (1978).
- [6] M. Salvatores, and G. Palmiotti, et al. “Resonance Parameter Data Uncertainty Effects on Integral Characteristics of Fast Reactors,” IAEA Specialist’s Meeting on Resonance Parameters, Vienna, 28 September - 2 October, 1981.
- [7] M. Herman, R. Capote, B.V. Carlson, P. Oblozinsky et al, “EMPIRE: Nuclear Reaction Model Code System for Data Evaluation”, *Nucl. Data Sheets* **108** (2007) 2655-2715
- [8] T. KAWANO and K. SHIBATA, “Covariance Evaluation System,” JAERI-Data/Code 97-037, Japan Atomic Energy Research Institute (1997) (n Japanese).
- [9] G. Rimpault, et al., “The ERANOS Code and Data System for Fast Reactor Neutronic Analyses,” Proc. Physor 2002 Conference, Seoul (Korea), October 2002.
- [10] SINBAD-2009.02: Shielding Integral Benchmark Archive and Database, Version February 2009, RSICC DATA LIBRARY DLC-237, ORNL
- [11] M.T. Pigni, M. Herman, C.M. Mattoon, et al. Evaluation of  $^{23}\text{Na}$  neutron cross sections for nuclear data assimilation, Wonder 2009 - Second International Workshop on Nuclear Data Evaluation for Reactor Applications - CEA Cadarache, 29th September - 2nd October, 2009 France.
- [12] G. Palmiotti, M. Salvatores, et. al., “A global approach to the physics validation

of simulation codes for future nuclear systems”, *Annals of Nuclear Energy* **36** (2009) 355–361.

[13] G. Palmiotti, M. Salvatores, H. Hiruta, “Sensitivity Analysis of Experimental Blanket/Reflector Interface Effects in Fast Reactors for Nuclear Data Improvement”, *Advances in Nuclear Fuel Management IV (ANFM 2009)*, Hilton Head Island, South Carolina, USA, April 12-15, 2009

[14] 3. R. E. Kaiser, J. M. Gasidlo, W. K. Lehto, L. A. Mountford, J. E. Powell, N. A. Hill, R. O. Vosburgh, and J. M. Stevenson, “ZPR3 Assemblies 53 and 54 – Continuation of Studies of Basic Physics Cores– Depleted Uranium Blanket and Iron Reflected Versions,” Reactor Physics Division Annual Report, July 1, 1968 to June 30, 1969, ANL-7610, pp.84-94